

# HaloSat Response Matrix Modifications

P. Kaaret and J. Bluem, 2022-01-28

## 1. Gain correction using spectra of Cas A

To check the on-orbit X-ray energy scale calibration, we examined spectra obtained while observing the supernova remnant (SNR) Cassiopeia A (Cas A). Cas A is chosen as a calibration target because of the strong emission lines present in its X-ray spectrum (Jahoda et al. 2006). The HaloSat field centered on Cas A includes another SNR, CTB 109, and several point sources, but the emission is dominated by Cas A.

### 1.1 Analysis and Results

We analyzed all of the observations of Cas A performed during the full HaloSat mission. Data were filtered using cuts on the VLE ( $> 7$  keV) count rate of 0.75 c/s and on the hard-band (3-7 keV) count rate of 0.12 c/s. We extracted one summed spectrum for each of the three DPUs (Figure 1) with channels grouped to have a minimum of 25 counts per bin. The instrumental background was modelled as a power law with a diagonal response matrix. We performed fits with the power law photon index calculated as described in Kaaret et al. (2020) and with the photon index for each DPU left as a free parameter. Emission from the cosmic X-ray background was modeled as the sum of an absorbed power law with fixed absorption, photon index, and normalization. The emission from Cas A was modeled as the sum of an absorbed power law with absorption fixed to  $1.47E21$  cm<sup>-2</sup> and a set of nine, narrow Gaussian emission lines. The set of lines used is the same as in Kaaret et al. (2019).

A response model was included in the fitting. Allowing the offset to vary while fixing the slope at unity improved the fit from  $\chi^2/\text{DoF} = 824.2/355$  to  $\chi^2/\text{DoF} = 437.5/352$ . Varying the slope while keeping the offset fixed to zero also improved the fit (to  $\chi^2/\text{DoF} = 452.9/352$ ), but the model with the varying offset is preferred. The best fitted model with varying offset is shown in Figure 1. The best fitted offsets with slope fixed at unity and 90% confidence uncertainties are given in Table 1. Allowing the instrumental background photon index to vary did not significantly improve the fit, giving  $\chi^2/\text{DoF} = 433.1/349$  corresponding to an F-test probability of 0.32. There was no significant change in the best fitted offsets (Table 2). Averaging the values and rounding to 1 eV, leads to an offset of 0.0232 keV for DPU14, 0.0240 keV for DPU54, and 0.0239 keV for DPU38. These offsets were tested using other HaloSat data sets.

Table 1: Response parameters using calculated background slope. Units are keV.

DPU	Offset	Lower error	Upper error
14	0.02320	-0.00191	+0.00074
54	0.02402	-0.00065	+0.00057
38	0.02393	-0.00063	+0.00054

Table 2: Response parameters using fitted background slope. Units are keV.

DPU	Offset	Lower error	Upper error
14	0.02316	-0.00181	+0.00075
54	0.02398	-0.00067	+0.00058
38	0.02389	-0.00064	+0.00055

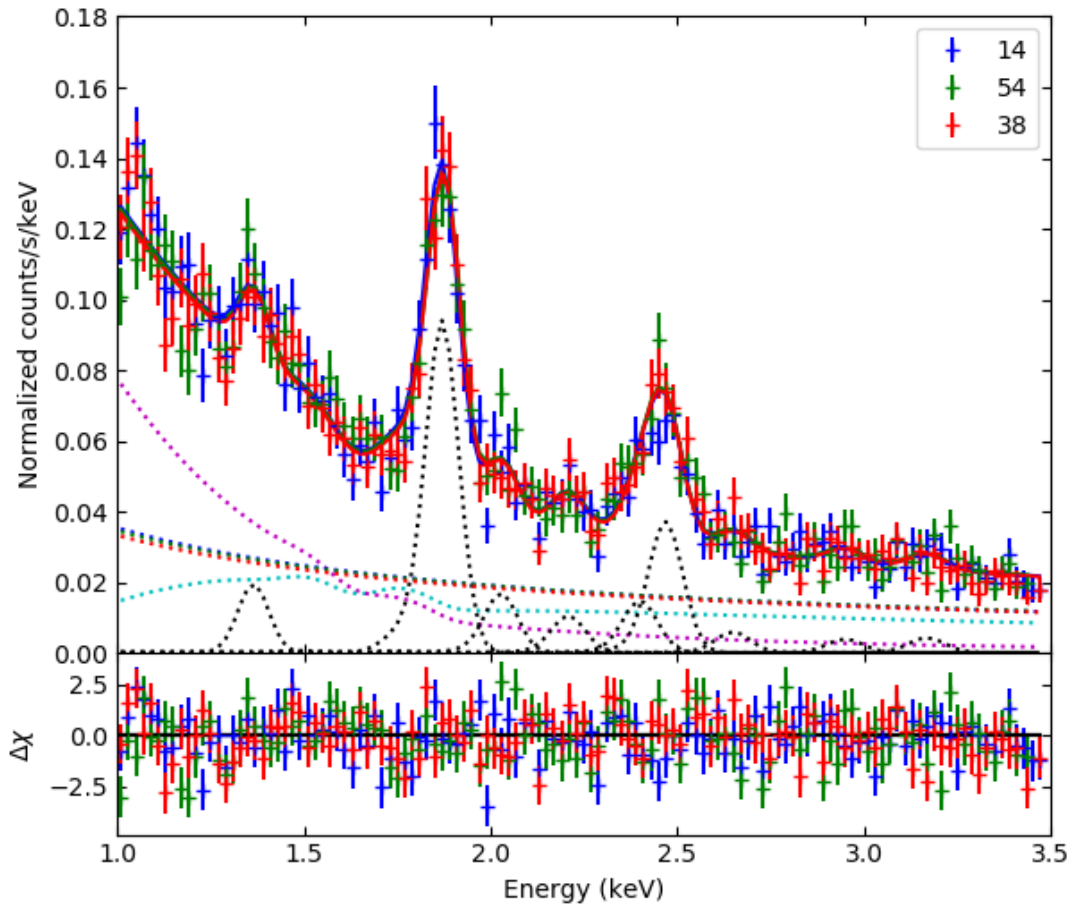


Figure 1: X-ray spectra of Cas A. Data are shown for all three DPUs: 14=red, 54=green, 38=red. The fitted instrumental background for each DPU is shown as a dotted curve with the same color as the data. The dotted cyan curve is the cosmic X-ray background. The dotted magenta curve is the power law from Cas A. The dotted black curves are the Gaussian emission lines.

## 1.2 Test using southern halo spectra

The new gain offset was testing using the southern halo data from Kaaret et al. (2020). Application of the gain offsets in Table 1 lead to:

- 1) No significant change in the Cash statistic. Median changed from 1.067 to 1.062.
- 2) A small change in the best fitted temperatures. The median change in kT is -0.0196 keV and the weighted average change is -0.0188 keV.
- 3) A moderate change in the best fitted emission measure (EM). The median of the fraction change in EM is 15% and 96% of fields have a fraction change in EM of less than 30%. The median of the change in EM divided by the statistical error on the EM is 0.67.

## 1.3 Test using stacked halo spectra

Spectra were produced by summing a large number of halo fields with consistent emission measure (see Bluem et al. 2022). Processing and background estimation were performed as described above. The spectra were fitted with a model consisting of an APEC model for the local hot bubble, an absorbed power law for the cosmic X-ray background, and two absorbed APEC models for the halo emission. Figure 2 shows the model fits with the original HaloSat gain values. Figure 3 shows the model fits with the gain corrections applied as listed in Table 2 and the Si edge as described in section 2. All spectra are rebinned for presentation using “setplot rebin 30 15”, for 30 sigma per bin with a cap of 15 channels combined. The gain corrections significantly improve the residuals of the fit. The fit statistic improved from  $\chi^2/\text{DoF} = 1266/973$  to  $\chi^2/\text{DoF} = 1069/973$ . The gain corrections produced a noticeable improvement from 0.45 keV to 0.8 keV. This had a significant effect on the model – the APEC temperatures before the gain are inconsistent with those found after.

## 1.4 Conclusions

We recommend use of an offset of 0.0232 keV for DPU14, 0.0240 keV for DPU54, and 0.0239 keV for DPU38 when using the HaloSat response files released on 2020-03-20.

The gain offset appears to have a modest effect on spectra with low statistics fitted with models with a single free component. However, the gain offset appears to be more consequential for spectra with high statistics and/or fits with multiple components.

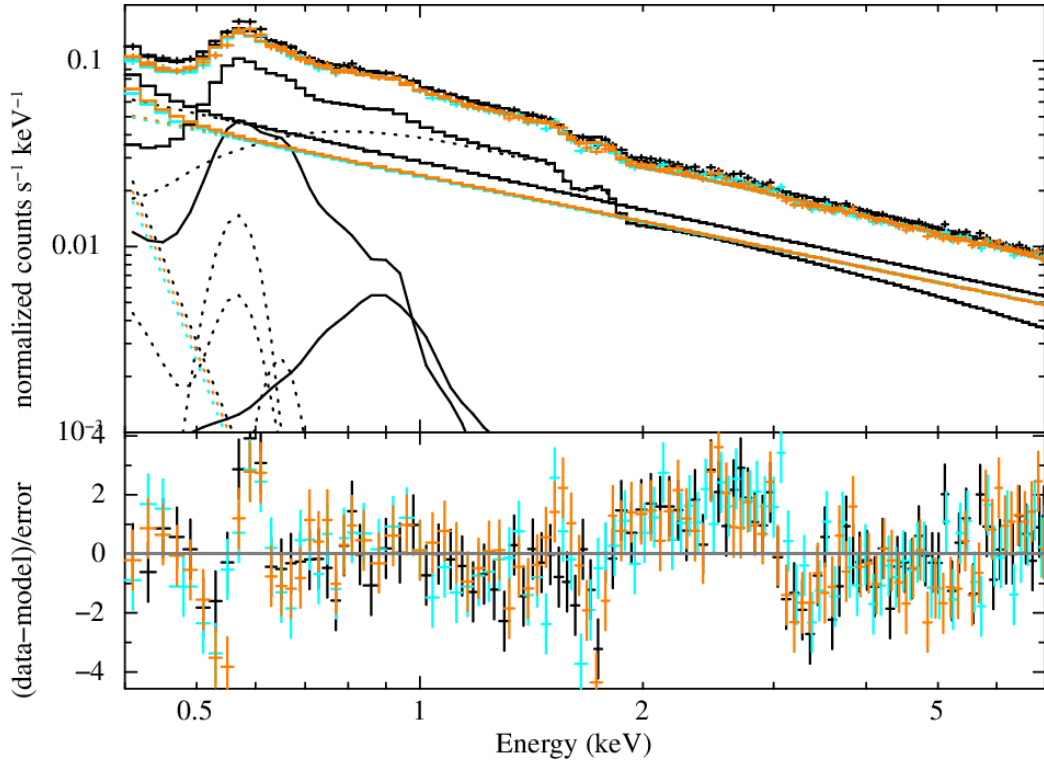


Figure 2: Stacked halo spectra before gain correction.

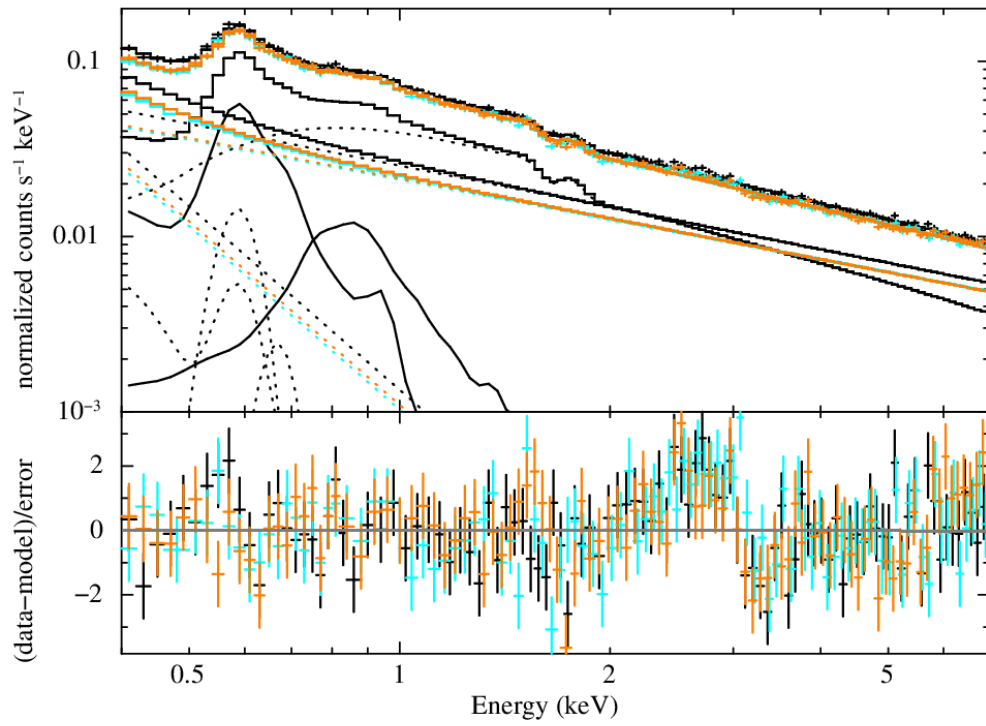


Figure 3: Stacked halo spectra after gain correction.

## 2. Investigation of edge features in the response using spectra of the Crab

To check incorrectly modeled edge features in the HaloSat response matrix, we examined spectra obtained while observing the Crab pulsar wind nebula and pulsar. The Crab is chosen for this purpose because it has a featureless X-ray spectrum. The emission within the HaloSat field centered on the Crab is dominated by the Crab.

### 2.1 Analysis and Results

We analyzed all of the observations of the Crab performed during the full HaloSat mission. Data were filtered using cuts on the VLE ( $> 7$  keV) count rate of 0.75 c/s and on the hard band (3-7 keV) count rate of 0.5 c/s. A Sun angle greater than  $100^\circ$  was required. The count rate threshold in the hard band is higher than typically used in HaloSat analysis because the Crab contributes significant flux in the hard band. We note that the feature around 3 keV induced by the standard hard rate cuts is not present in the Crab spectra. We extracted one summed spectrum for each of the three DPUs (Figure 1) with channels grouped to have a minimum of 25 counts per bin. The gain corrections described in the previous section were applied. The instrumental background was modelled as a power law with a diagonal response matrix. The normalization and photon index for each DPU left as free parameters. The instrumental background photon index calculation described in Kaaret et al. (2020) are not applicable due to the non-standard data filtering required for the Crab. Emission from the cosmic X-ray background (CXB) was modeled as an absorbed power law with fixed absorption, photon index, and normalization. Emission from the Local Hot Bubble (LHB) was modeled as an unabsorbed APEC. The parameters for the CXB and LHB were set following Kaaret et al. (2020). The emission from the Crab was modeled as an absorbed power law. The absorption column density and power law photon index and normalization were allowed to vary.

Figure 4 shows the spectra for all three detectors. The spectral fits show strong residuals near 1.8 keV which we identify as the silicon K edge. The fit has  $\chi^2/\text{DoF} = 1424.38/978$ . Figure 5 shows the spectral fits including an edge (model 'edge' in Xspec) with the edge energy fixed to 1.839 keV for silicon. The maximum optical depth ( $\tau$ ) is linked between the detector and the best fit value is  $\tau = -0.169 \pm 0.014$ . Addition of the edge significantly improves the fit to  $\chi^2/\text{DoF} = 1084.85/977$ . The corresponding F-test probability is  $9\text{E-}60$ . Allowing  $\tau$  to vary between detectors produces no significant improvement in the fit (F-test probability = 0.38). The error ranges on the  $\tau$  values for the individual detectors all include the linked fit value of  $\tau = -0.169$ .

### 1.4 Conclusions

We recommend inclusion of a negative absorption edge using the Xspec edge model with a threshold energy of 1.839 keV and  $\tau$  of 0.169 when using the HaloSat response files released on 2020-03-20.

We note that the edge is ‘negative’. This means that there is less absorption than included in the current response model. An Si thickness of 0.24 microns produces a step in transmission across the Si K edge equivalent to the measured tau. Such a change in Si thickness should also affect the transmission at low energies, but this is not observed. The equivalent Si thickness is comparable to the thickness of front layer (0.11 microns) and incomplete charge collection layer (0.20 microns) of the HaloSat silicon drift detectors (Zajczyk et al. 2020, *J. Astron. Telesc. Instrum. Syst.* 6, 044005-1). The edge may result from incomplete modeling of the interactions of the Auger and photo-electrons in those regions (Scholze and Procop 2009, *X-Ray Spectrom.* 38, 312).

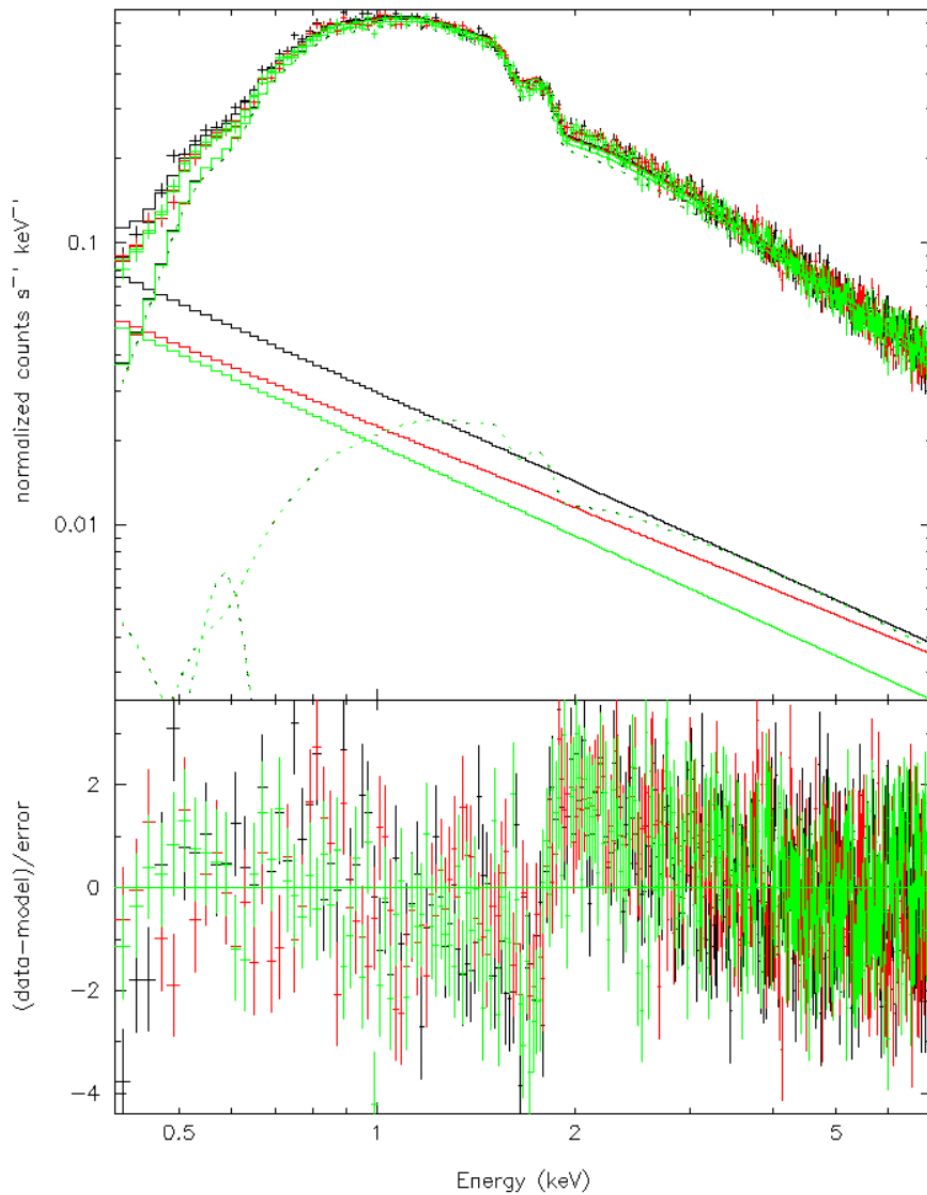


Figure 4: Crab spectrum before inclusion of the negative Si edge. There are strong residuals around 1.8 keV.

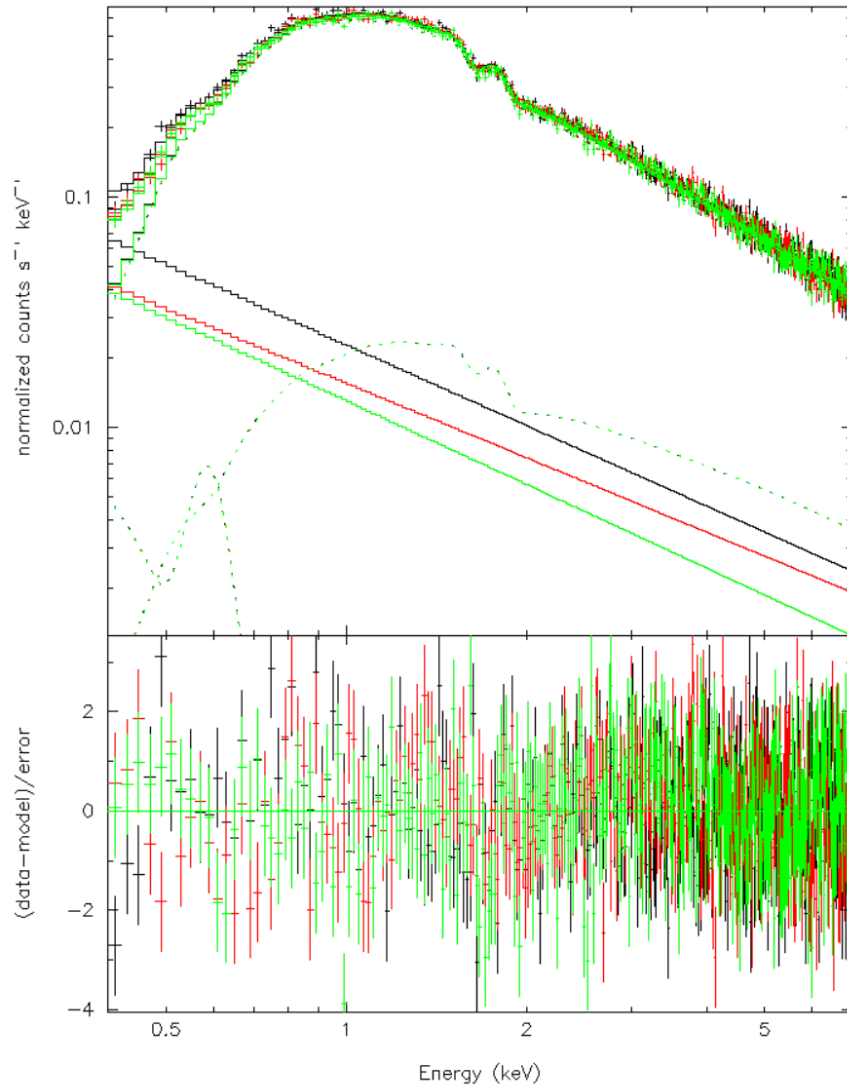


Figure 5: Crab spectrum with inclusion of a negative Si edge. The residuals around 1.8 keV are greatly improved.